Available online at www.sciencedirect.com
ScienceDirect
Estuarine, Coastal and Shelf Science 73 (2007) 175–187
ESTUARINE COASTAL AND SHELF SCIENCE
www.elsevier.com/locate/ecss

Anthropogenic influence on sedimentation and intertidal mudflat change in San Pablo Bay, California: 1856–1983

Bruce E. Jaffe [a,*], Richard E. Smith [b,1], Amy C. Foxgrover [a]

[a] U.S. Geological Survey Pacific Science Center, Santa Cruz, CA 95064, USA
[b] U.S. Geological Survey, Menlo Park, CA 94025, USA

Received 15 February 2007; accepted 18 February 2007
Available online 19 April 2007

Abstract

Analysis of a series of historical bathymetric surveys has revealed large changes in morphology and sedimentation from 1856 to 1983 in San Pablo Bay, California. In 1856, the morphology of the bay was complex, with a broad main channel, a major side channel connecting to the Petaluma River, and an ebb-tidal delta crossing shallow parts of the bay. In 1983, its morphology was simpler because all channels except the main channel had filled with sediment and erosion had planed the shallows creating a uniform gently sloping surface. The timing and patterns of geomorphic change and deposition and erosion of sediment were influenced by human activities that altered sediment delivery from rivers. From 1856 to 1887, high sediment delivery (14.1×10^6 m^3/yr) to San Francisco Bay during the hydraulic gold-mining period in the Sierra Nevada resulted in net deposition of $259 \pm 14 \times 10^6$ m^3 in San Pablo Bay. This rapid deposition filled channels and increased intertidal mudflat area by 60% (37.4 ± 3.4 to 60.6 ± 6.2 km^2). From 1951 to 1983, $23 \pm 3 \times 10^6$ m^3 of sediment was eroded from San Pablo Bay as sediment delivery from the Sacramento and San Joaquin Rivers decreased to 2.8×10^6 m^3/yr because of damming of rivers, riverbank protection, and altered land use. Intertidal mudflat area in 1983 was 31.8 ± 3.9 km^2, similar to that in 1856. Intertidal mudflat distribution in 1983, however, was fairly uniform whereas most of the intertidal mudflats were in the western part of San Pablo Bay in 1856. Sediment delivery, through its affect on shallow parts of the bay, was determined to be a primary control on intertidal mudflat area. San Pablo Bay has been greatly affected by human activities and will likely continue to erode in the near term in response to a diminished sediment delivery from rivers.

Keywords: sedimentation; bathymetry; long-term changes; intertidal flats; tidal flats; estuary; USA; California; San Francisco Estuary; San Francisco Bay; San Pablo Bay

1. Introduction

The spatial and temporal distribution of sedimentation, including the processes of deposition, transport, and erosion, is fundamental information for making sound decisions on a wide variety of management issues for estuaries. Sedimentation changes bathymetry and therefore habitat extent and distribution. Bathymetric changes, in turn, affect flow patterns and tidal exchange, which are important in sediment, salt, larval, and nutrient transport (e.g., Uncles and Peterson, 1996; Monismith et al., 2002). Predicting natural and anthropogenic changes to ecosystems and designing successful restoration projects require knowledge of patterns of deposition and erosion. For example, intertidal mudflat extent is controlled by sedimentation. Planning maintenance of shipping channels and disposal sites for dredged material is better done with the knowledge of the distribution of natural sediment accumulation and erosion. Contaminant transport and cycling are also influenced by sedimentation (Marvin-DiPasquale et al., 2003; Schoellhamer et al., 2003). Deposition of clean sediment can isolate contaminated sediment, or conversely, erosion may expose contaminated sediments deposited at some time in the past (Higgins et al., 2005, 2007). At a longer time scale, planning for estuarine ecosystem change requires understanding

* Corresponding author.
E-mail address: bjaffe@usgs.gov (B.E. Jaffe).
[1] Retired.

0272-7714/$ - see front matter © 2007 Elsevier Ltd. All rights reserved.
doi:10.1016/j.ecss.2007.02.017

how natural changes in the environment (e.g., sea-level rise, drought periods) and human activities, such as water management, affect sedimentation.

Although knowledge of long-term trends in deposition and erosion are important for proper management of estuarine ecosystems, it is difficult to gain this knowledge from short field experiments or other traditional methods. A long-term, large-scale perspective of the sediment system is possible, however, by analyzing a long sequence of bathymetric surveys.

This paper presents a history of bathymetry, deposition, erosion, and intertidal flat change in San Pablo Bay, California from 1856 to 1983 and relates it to changes in sediment delivery to the bay. This history was developed using computer analysis and display of hydrographic and topographic surveys made by the U.S. Coast and Geodetic Survey and the National Ocean Service (NOS). This study is not the first one addressing bathymetric change in San Pablo Bay (Gilbert, 1917; Smith, 1965; Ogden Beeman and Associates and Ray Krone and Associates, 1992) but is the most comprehensive to date.

2. Setting

San Pablo Bay is a circular bay in the northern part of the San Francisco Estuary, California (Fig. 1). The bay is shallow – two-thirds of it is less than 2 m deep at mean lower low water (MLLW). The average depth of San Pablo Bay at mean tide is 3.7 m. A deep (11–24 m, average 12 m) main channel in its southern part connects Central San Francisco Bay in the west to Carquinez Strait in the east. This channel, which averages about 2.5 km in width, is an important control on San Pablo Bay's hydrodynamic regime (Gartner and Yost, 1988) and sediment-delivery pattern (Ruhl et al., 2001).

Winds are predominantly northwesterly and are strongest during the spring and summer, with average wind speeds of approximately 3 m/s on the west shore (Hayes et al., 1984). Winter storms, which occur about twice a month, cause southeasterly and southerly winds that can exceed 18 m/s in velocity (Conomos and Peterson, 1976). Diurnal winds are strongest during the summer, with typical afternoon wind speeds of 9 m/s, which is three times faster than morning winds (Miller, 1967).

Forcing at time scales ranging from seconds to decades influences the hydrodynamic regime of San Pablo Bay. Waves generated by moderate winds have heights of 0.5 m and periods of 2 s (Klingeman and Kaufman, 1965). Because of the short wave periods, wave orbital velocities decay rapidly with depth and interact with the bottom only in the shallow parts of the bay (e.g., water depths of less than 3 m for a 2 s period wave). Winter storms can generate larger waves with periods of 5 s in the San Francisco Bay system (Putnam, 1947). Besides generating waves, winds generate mean currents that persist for hours or days. At a longer time scale, tides and tidal currents are important. Tides in San Pablo Bay are mixed semidiurnal (form numbers of 0.71–0.77; Cheng and Gartner, 1984). Tidal currents are greatest in the main channel, with spring tide velocities of more than 1 m/s, decreasing in shallower water to 0.4 m/s in 2-m water depth (Cheng and Gartner, 1984; Gartner and Yost, 1988). The average tidal range is 1.8 m (National Oceanic and Atmospheric Administration, 1986). Water level in the study area also varies at a longer time scale. Sea level, measured by a tide gauge near the entrance to the San Francisco Estuary (Golden Gate) (Lyles et al., 1988), rose at an average rate of about 1.3 mm/yr, or about 17 cm, during the period of hydrographic surveys (1856–1983).

Bottom-sediment grain size in San Pablo Bay reflects local hydrodynamics and sediment source. Median grain size ranges from 2.3 μm at a low-energy point in the center of the bay to 430 μm in the energetic main channel near Carquinez Strait (Locke, 1971). Except for the main channel and several shallow areas, sediment consists predominantly of mud – more than half of the bay contains sediment with a median grain size of less than 5 μm.

Sediment deposited in San Pablo Bay is transported from the Sacramento and San Joaquin Rivers (after passing through

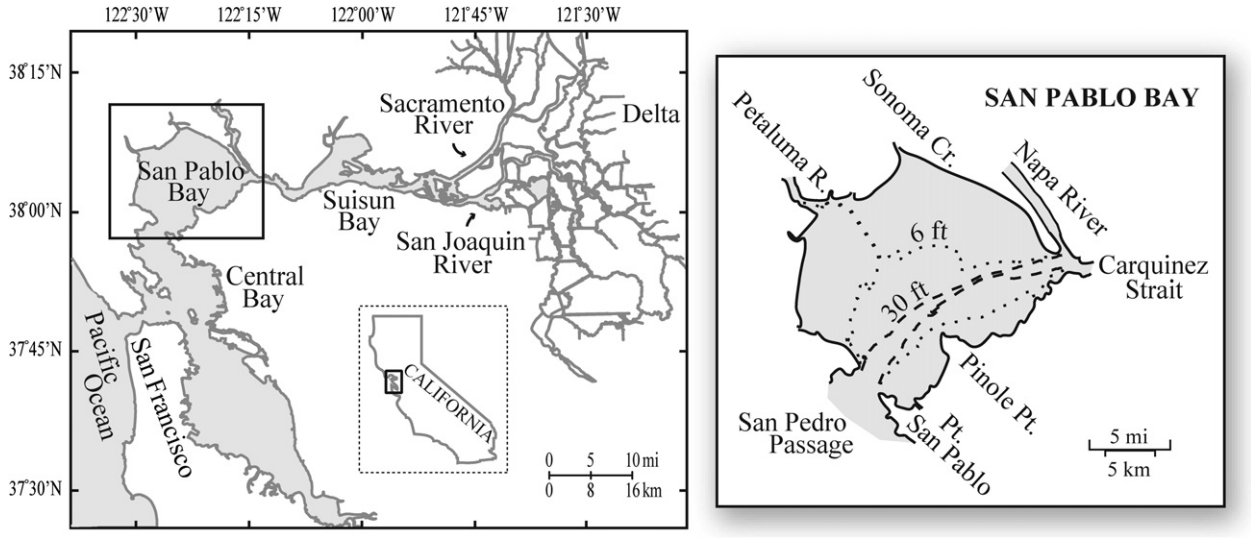

Fig. 1. Location of study area in the San Francisco Estuary, California.

Suisun Bay and Carquinez Strait), from Central San Francisco Bay, and from local streams. From 80 to 90% of the sediment reaching the San Francisco Estuary is delivered by the Sacramento and San Joaquin Rivers (Smith, 1965; Krone, 1979; Porterfield, 1980).

3. Methods

Data from six bathymetric surveys were modeled using surface modeling software with similar methods as have been reported by Sherwood et al. (1990), Hopkins et al. (1991), List et al. (1994), Jaffe et al. (1998), Cappiella et al. (1999), and Gibbs and Gelfenbaum (1999). A continuous surface representation (surface grid) of each bathymetric survey was created by using Topogrid, an ArcInfo module that utilizes a discretised thin plate spline interpolation technique (Wahba, 1990). Topogrid is designed for modeling drainage basins and represents estuarine morphology well. Input data were a combination of point soundings and hand-drawn depth contours (Jaffe et al., 1998). Topogrid uses an iterative interpolation technique where the contours are first used to establish general morphology of the surface and then both contours and point soundings are used to refine the grid. Each historical bathymetric surface is defined by more than 300,000 grid cells (each 50-m square).

Creation of accurate surface grids involved several steps (Jaffe et al., 1998). For the 1856, 1887, 1898, and 1922 surface grids, data were taken from Mylar copies of the original 1:20,000 NOS Hydrographic Sheets (H-sheets). Contours from these sheets were checked for accuracy, and additional contours were added in areas where point soundings were sparse. The annotated H-sheets were scanned and registered to a common horizontal datum (NAD27), using latitude/longitude graticules and hard shoreline features on a National Wetlands Inventory digital map (http://wetlands.fws.gov/). Point soundings and depth contours were digitized from the registered image. For the 1951 and 1983 surface grids, digital soundings from the NOS Geophysical Data System for Hydrographic Survey Data (National Oceanic and Atmospheric Administration, GEODAS v. 3.3) were used. For all years, input data were gridded, and the grids were compared with the input data to check for problem areas. The final step was another gridding after adding point soundings and contours so as to force grids to accurately represent historical bathymetry.

Once surface grids were revised to meet an acceptable level of error, change grids were generated by differencing surface grids and applying a vertical correction to bring surveys to a common vertical datum. The vertical correction was necessary because MLLW, the reference for soundings of each bathymetry survey, was not constant because of relative sea-level change and different averaging periods for the tidal data. In general, the averaging period was 19 years, which is the 18.6-year tidal epoch extended to an entire year to remove bias from seasonal water level fluctuation. However, tidal records in San Pablo Bay were not continuous for the entire study period, and it was necessary to use the longer tidal record at the Golden Gate tide station to determine vertical-datum corrections (Dedrick, 1983; Jaffe et al., 1991). These change grids were used to identify patterns of change and to calculate the volumes and rates of deposition, erosion, and net sedimentation for each survey period.

4. Error analysis

4.1. Grid errors

Two types of error are associated with the grids – bias and random error. Bias enters from inaccuracies in determining the relation of MLLW datums for different surveys and from grid representation differing from the sounding values because of modeling algorithms. Random error is associated with sounding inaccuracy. Sounding errors are randomly distributed in space and independent of each other.

Uncertainty in the MLLW datum varies with the calculation method. For the last two bathymetric surveys, 1951 and 1983, MLLW datums are known (calculated from data collected for a tidal epoch at the long-term tide station near the Golden Gate). For the first bathymetric survey, in 1856, a 2-month average of MLLW measured at temporary tide staffs located in San Pablo Bay was used, and the relation of this datum to subsequent datums is more uncertain. By examining tidal records at the Golden Gate tide station, which was operational during the 1856 bathymetric survey, the relation of the 1856 datum to the datums used in later surveys can be estimated. For example, the 1887 H-sheets include notes indicating that a temporary tide station was operational in San Pablo Bay during the survey (February and March). If this 2-month-long record was used to establish the MLLW datum, and the tides behaved similarly to those at the Golden Gate, the datum would be 1.68 m (values from the Golden Gate tide staff used for reference). An alternative method for calculating the MLLW datum is to compare simultaneous measurements at the temporary tide station in San Pablo Bay with those at the Golden Gate tide station to establish a 19-year epoch (Swanson, 1974). This method yields an MLLW datum of 1.64 m referenced to the Golden Gate tide staff. The difference between the two methods is 0.040 m. To be conservative, because we do not know which method was used, we assume the error in the MLLW datum from 1856 to 1887 to be 0.040 m. Using similar reasoning, the errors in the MLLW datums for the periods 1887–1898, 1898–1922, and 1922–1951 are 0.094, 0.061, and 0.006 m, respectively.

The second source of bias, grid representation differing from the sounding values because of modeling algorithms, was estimated by comparing the modeled surface to original soundings. The average bias for all soundings during each survey period ranged from −0.07 to −0.01 m. The magnitude of this error indicates how well the grids honor the soundings. The difference between grid bias for each survey period is included in the error for net sedimentation even though it was removed.

The magnitudes of sounding errors are larger than the biases. Because sounding errors are random and have a zero mean, they do not influence estimates of net sedimentation. The sum of a large group of soundings that are both deeper and shallower than the actual depths results in cancellation of error and

a true average depth, although, each individual sounding contains some errors. The error criteria for bathymetric surveys have changed over time (Adams, 1942; Schalowitz, 1964; Sallenger et al., 1975). For example, in the early surveys, sounding error, determined by comparing independent estimates at trackline crossings, was not allowed to exceed 8 cm in water depth of less than 1.5 m. Trackline-crossing errors were examined in the field. Lines with trackline-crossing errors exceeding the error criteria were resurveyed (Schalowitz, 1964).

4.2. Intertidal mudflat area error

The error in intertidal mudflat area was estimated by assuming that MLLW (bayward edge of intertidal mudflat) could be either 0.076 m (1/4 foot) too deep or too shallow. This estimate is conservative – the actual error is probably less because of stringent sounding-error criteria for shallow soundings (Schalowitz, 1964; Sallenger et al., 1975).

5. Results

5.1. Historical bathymetric and sedimentation change in San Pablo Bay

San Pablo Bay changed markedly between 1856 and 1983. The resultant changes in morphology and sedimentation patterns are depicted in images of the bathymetry and sedimentation grids, which are based on more than 215,000 depth soundings (Fig. 2a, b).

5.1.1. Change from 1856 to 1887

In 1856, San Pablo Bay had a complex morphology with several channels and small river deltas (Figs. 2a and 3). A broad main-channel system connected the Point San Pedro pass (offshore of San Pablo Point) in the west to Carquinez Strait in the east. The main-channel system had a northern branch (average depth, approximately 8 m; maximum depth, 12 m) and a more developed southern branch (average depth, approximately 13 m; maximum depth, 27 m). The channel system had a maximum width of 5 km (Figs. 2a and 3). A well-developed channel connected the main channel to the Petaluma River in the northwest. An ebb-tidal delta offshore of Sonoma Creek restricted exchange between it and the bay (Figs. 1 and 2a). From 1856 to 1887, San Pablo Bay filled by $259 \pm 14 \times 10^6$ m^3 (average rate of $8.3 \pm 0.4 \times 10^6$ m^3/yr) as massive volumes of sediment released by hydraulic gold mining in the Sierra Nevada foothills entered the bay (Table 1, Fig. 2b). This influx of sediment decreased depth by an average of about 85 cm. Almost the entire bay was depositional (89%, Table 1). Parts of the main-channel margin accreted more than 4 m as it narrowed (Figs. 2a, b and 3). The primary erosional areas were the deepest part of the main channel, deeper parts of the channels in the west, and an ebb-tidal delta offshore of Sonoma Creek.

5.1.2. Change from 1887 to 1898

San Pablo Bay likely continued to fill from 1887 to 1898 (Fig. 2a, b), although the error in estimates of net sedimentation allows for possible net erosion. The rate of net sedimentation, $1.0 \pm 3.4 \times 10^6$ m^3/yr, decreased markedly from the earlier period (Table 1). A major factor in slowing sedimentation was the outlawing in 1884 of discharge of hydraulic-mining debris to rivers, which greatly reduced the volume of sediment entering the Sacramento–San Joaquin River Delta (hereafter referred to as the Delta) and San Francisco Bay. The main channel deepened and narrowed (Figs. 2a, b and 3). Side channels continued to fill, decreasing the connection between the bay and rivers. For example, the channel offshore of the Petaluma River decreased in width from 3.4 to 2.3 km at its bayward limit during this period as a reduced tidal prism caused by diking of tidal marshes resulted in a decreased shear-stress in the bottom of the channel, which favors deposition (see Friedrichs, 1995 for a theoretical treatment of this process). Shallows in the western part of the bay changed from depositional to either stable or erosional (Fig. 2b). Overall, about half of the bay was depositional, and half was erosional (Table 1).

5.1.3. Change from 1898 to 1922

From 1898 to 1922, a net volume of $41 \pm 20 \times 10^6$ m^3 of sediment, an average rate of $1.7 \pm 0.9 \times 10^6$ m^3/yr, was deposited in San Pablo Bay (Table 1). During this period, approximately two-thirds of the bay was depositional, especially in the shallow areas (<2-m depth) (Fig. 2b). The channel extending from the Petaluma River filled to a point where dredging (indicated by straight path with a dogleg cutting through intertidal mudflat, Fig. 2a) was required to allow ships to travel upriver. The primary erosional areas were the western shallows and the main channel, which continued to deepen (Figs. 2a, b and 3).

5.1.4. Change from 1922 to 1951

From 1922 to 1951, the rate of net sedimentation in San Pablo Bay was similar to the rate during the preceding 24 years. A net volume of $52 \pm 3 \times 10^6$ m^3 of sediment, an average rate of $1.8 \pm 0.1 \times 10^6$ m^3/yr, was deposited. The shallows were primarily depositional, and most erosion occurred in vicinity of the main channel; overall, about two-thirds of the bay was depositional. The straight section of the 30-foot contour lines in the southeast delineates an area of dredging (less than a quarter the length of the main channel). The center of the main channel continued to deepen (Figs. 2a, b and 3).

5.1.5. Change from 1951 to 1983

San Pablo Bay lost sediment overall from 1951 to 1983 in contrast to the previous ~100 years when the bay was filling with sediment. A net volume of $23 \pm 3 \times 10^6$ m^3 of sediment, an average rate of $0.7 \pm 0.1 \times 10^6$ m^3/yr, eroded from San Pablo Bay (Table 1). More than two-thirds of the bay (70%, Table 1) was erosional with the northern and northeastern shallows and the margins of the main channel depositional. Klingeman and Kaufman (1965) also observed deposition on the main-channel margins in a short study that used naturally occurring radioactive tracers. Dredging of the main channel near Pinole Point averaged about 0.2×10^6 m^3/yr from 1955 to 1983 (Ogden Beeman and Associates and Ray Krone and Associates, 1992) and is easily identified by the straight 30-foot contours in Fig. 2a. The dredged material was disposed

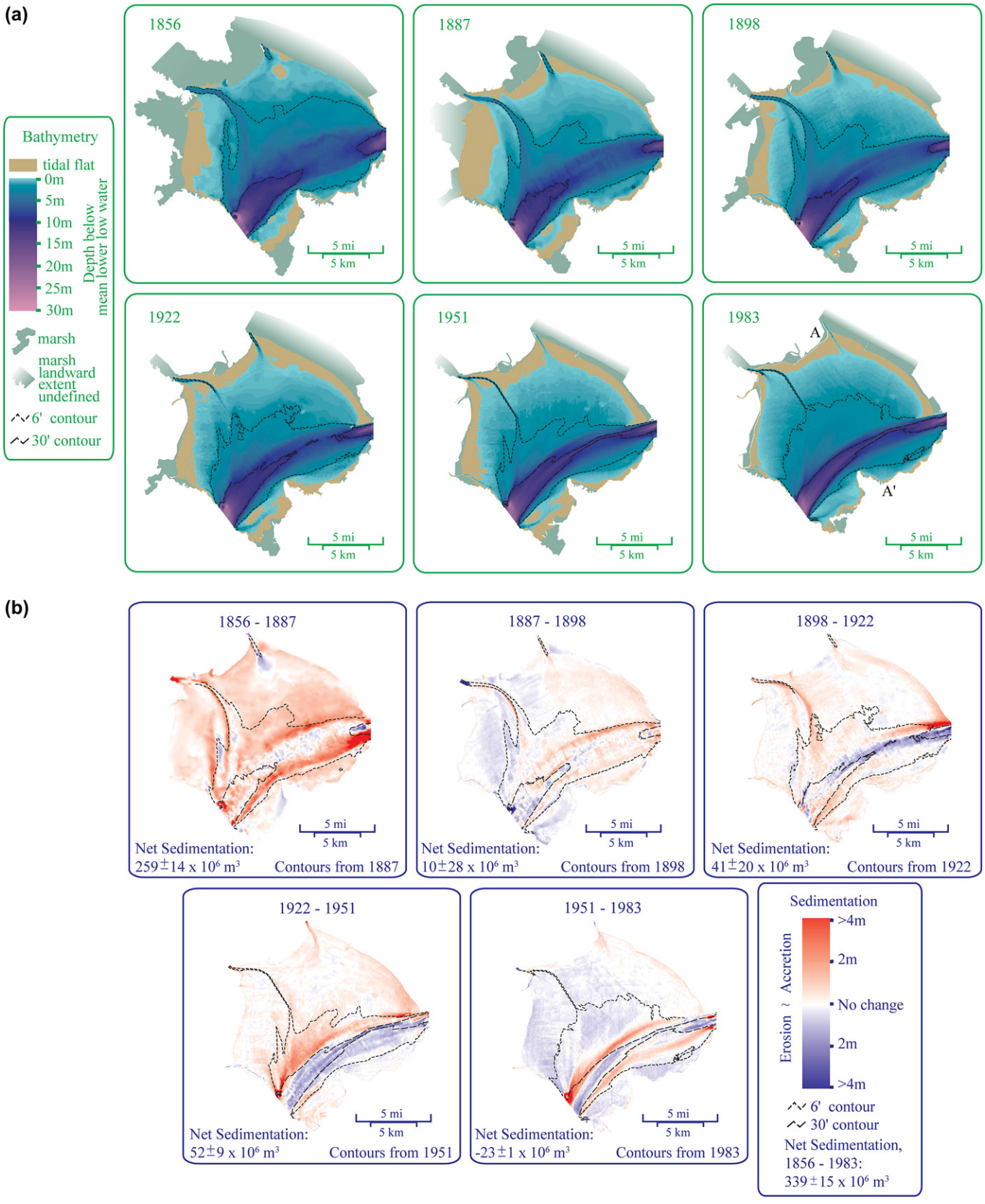

Fig. 2. (a) Color-shaded bathymetry maps of San Pablo Bay for 1856–1983, (b) color-shaded sedimentation maps of San Pablo Bay for 1856–1983. An overall decrease in depth of the bay is shown by lighter green colors in (a) and migration of the 6-foot contour bayward. The massive accretion during the hydraulic-mining period is shown in the 1856–1887 period in (b) by red shading. The erosion during the 1951–1983 period, which occurred as damming of rivers increased and land use changed, is shown by blue shading.

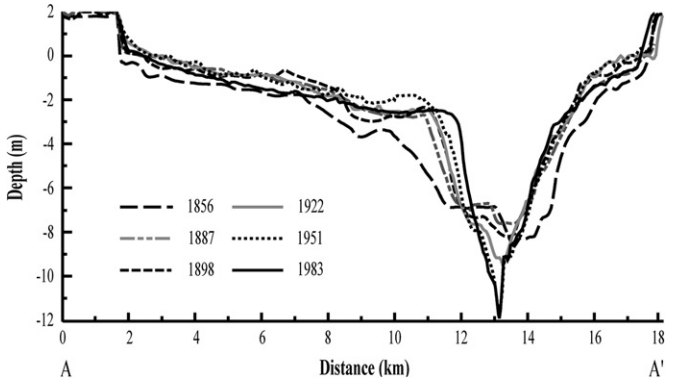

Fig. 3. Profile of San Pablo Bay floor along line A–A′ (Fig. 2a) for period 1856–1983. Note that main channel has narrowed and deepened and shallows have filled over time. Most of this change occurred from 1856 to 1887 when hydraulic mining resulted in unusually high sediment delivery to San Pablo Bay.

within San Pablo Bay and did not contribute to the net loss of sediment.

5.2. A simple model for sedimentation in San Pablo Bay

Net sedimentation in San Francisco Bay results from the difference between sediment delivery from rivers, primarily through episodic flood deposition, and sediment loss from wind, wave, and tidal processes that erode the bay (Krone, 1979). A simple model for sedimentation in San Pablo Bay is that processes controlling sediment loss have not varied greatly over time and the net sedimentation reflects fluctuations in delivery rate.

The rate of sediment delivery to San Pablo Bay has changed over time in response to human activities. For instance, delivery rate increased greatly beginning in the 1850s as debris from hydraulic gold mining in the Sierra Nevada foothills was transported to the bay. Gilbert (1917, p. 67) estimated that sediment delivery before hydraulic mining "amounted to perhaps 2 million cubic yards per year" (1.5×10^6 m^3/yr). Approximately 1.675×10^9 m^3 of hydraulic-mining debris was created from 1849 to 1909 (Gilbert, 1917, p. 43). Although the coarser fraction remained in the foothills, filling stream valleys by as much as 10 m (Gilbert, 1917), the finer fraction, silt and clay, was carried to the bay quickly by the Sacramento and San Joaquin Rivers. Gilbert (1917, p. 50) estimated that 1.146×10^9 m^3 of sediment (average rate of 14.1×10^6 m^3/yr) was transported to San Francisco Bay between 1849 and 1914. This is approximately 70% of the debris created by hydraulic mining (Gilbert, 1917, p. 46).

The California Supreme Court (Sawyer Decision) stopped discharge of mine tailings to rivers in 1884 resulting in a great decrease in the rate of sediment delivery by the early 1900s. Porterfield (1980, Table 20) estimated that the Sacramento and San Joaquin Rivers delivered an average of 5.04×10^6 metric tons/yr (5.90×10^6 m^3/yr, using his estimate of bulk sediment density of 53.2 lb/ft^3 [0.85 g/cm^3]) of sediment to San Francisco Bay from 1909 to 1959. Smith (1965) estimated a similar, but lower, sediment delivery to the bay for the period 1924 to 1960 of 4.04×10^6 metric tons/yr (4.74×10^6 m^3/yr, assuming a bulk sediment density of 0.85 g/cm^3). The delivery rate continued to decrease in the late 1900s. An average of 2.38×10^6 metric tons/yr (2.79×10^6 m^3/yr, assuming a bulk sediment density of 0.85 g/cm^3) of sediment was delivered to the bay from 1956 to 1990 (Ogden Beeman and Associates and Ray Krone and Associates, 1992, Table 5).

The decrease in the sediment-delivery rate during the late 1900s has multiple causes, including damming of rivers. From the 1940s to the 1970s, many dams were built to meet California's need for water (Porterfield, 1980). One consequence of dam building was a decrease in sediment delivery to the San Francisco Estuary (McKee et al., 2006; Wright and Schoellhamer, 2004). Sediment delivery is decreased not only by trapping sediment behind the dam but also by decreasing peak flows on the river, diminishing their capacity to transport sediment stored in the river system. Sediment transport is related to flow speed to the third or fourth (or higher) power (Van Rijn, 1993), and so decreasing flow speed greatly affects sediment transport and supply downstream. The volume of sediment trapped behind reservoirs on tributaries of the Sacramento River from 1940 to 2001 was greater than the decrease in suspended-sediment transport in the Sacramento River about 100 km below the dams during that same period (Wright and Schoellhamer, 2004). During this period and earlier, other human activities impacted sediment delivery to the San Francisco Estuary (Wright and Schoellhamer, 2004). Rivers were channelized, decreasing the sediment loss to flood plains and marshes, and riverbanks were stabilized, decreasing the sediment gain from riverbank erosion. Logging, urbanization, agriculture, and grazing increased sediment loads. The last two hydrographic surveys of San Pablo Bay (1951 and 1983) correspond to a period when damming and other human activities had caused a net decrease in sediment delivery to the San Francisco Estuary (Krone, 1979; Wright and Schoellhamer, 2004; McKee et al., 2006).

Comparison of net sedimentation and rate of sediment delivery in San Pablo Bay indicates similar trends (Fig. 4a).

Table 1
History of deposition, erosion, and net sedimentation in San Pablo Bay

Period	Net sedimentation (10^6 m^3)	Sedimentation rate			Surface area		
		Net (10^6 m^3/yr)	Deposition (10^6 m^3/yr)	Erosion (10^6 m^3/yr)	Total (km^2)	Percent depositional	Percent erosional
1856–1887	259 ± 14	8.3 ± 0.4	8.8	−0.4	304	89	11
1887–1898	11 ± 36	1.0 ± 3.4	5.5	−4.5	296	54	46
1898–1922	41 ± 20	1.7 ± 0.9	3.5	−1.8	290	63	37
1922–1951	52 ± 3	1.8 ± 0.1	3.4	−1.6	280	68	32
1951–1983	-23 ± 3	-0.7 ± 0.1	1.7	−2.4	275	30	70

Annually, the volume of sediment deposited appears to be approximately 3×10^6–5×10^6 m^3 less than the sediment delivery from the Sacramento and San Joaquin Rivers and local streams (local stream sediment delivery was about 0.3×10^6 m^3/yr during the first part of the 20th century; Porterfield, 1980). The decrease in sediment delivery resulted in net erosion for the last time period, 1951–1983. This erosion, as well as changes in sedimentation during earlier periods, was reflected in morphologic change, including change in intertidal mudflats.

5.3. Intertidal mudflat change

The intertidal mudflat area in San Pablo Bay changed from 1856 to 1983 in response to sediment-delivery fluctuations (Fig. 4a, b). The abundant supply of sediment from hydraulic mining resulted in deposition in the shallows and a 60% increase in intertidal mudflat area (37.4 ± 3.4 to 60.6 ± 6.6 km^2) from 1856 to 1887.

The distribution of intertidal mudflats also changed significantly over time. In 1856, intertidal mudflats in the northern, eastern, and southeastern parts of the bay were narrow. These intertidal mudflats, as well as the one in the western part of the bay, widened from 1856 to 1887. From 1887 to 1898, land reclamation on the west shore of the bay and natural processes elsewhere in the bay decreased its intertidal mudflat area by about 15 ± 6 km^2 (Fig. 2a). Intertidal mudflat loss in the western and northern parts of the bay and gain in the eastern part of the bay resulted in a fairly uniform intertidal mudflat width in 1951 (Fig. 2a). Erosion resulted in a decrease in intertidal mudflat area from 58.0 ± 10.2 km^2 in 1951 to 31.7 ± 3.9 km^2 in 1983, an average loss of 0.82 km^2/yr from 1951 to 1983.

5.4. Sedimentation in similar dynamical regions

Bay-averaged net sedimentation, though indicative of the general state of San Pablo Bay, does not describe the distribution and size of depositional and erosional areas. This information is exploited in an analysis of similar dynamical regions to assess sedimentation processes and sediment transport pathways. Here we used the patterns of deposition and erosion, and the spatial variation of tidal and wind–wave energy, to define 11 regions with coherent behavior (Fig. 5). Shallows extended to a depth of about 1.8 m and were divided into five regions, with boundaries at creeks or headlands. Boundaries of the other six regions were allowed to change over time to follow edges of large areas with either deposition or erosion.

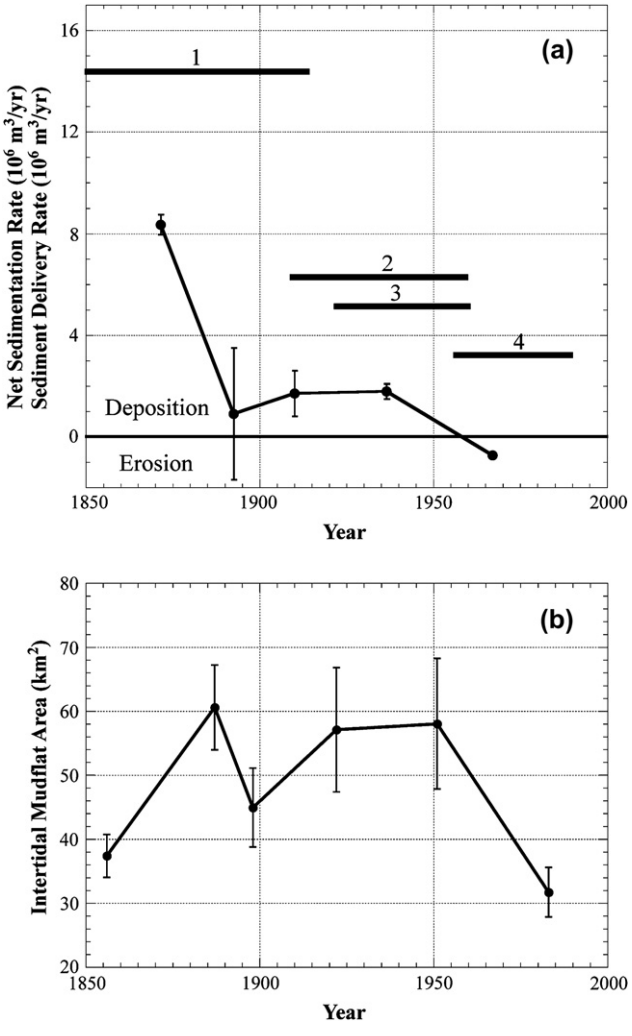

Fig. 4. (a) Net sedimentation and (b) intertidal mudflat area in San Pablo Bay from 1856 to 1983. Horizontal lines are sediment-delivery estimates: 1, Gilbert (1917) for 1850–1914; 2, Smith (1965) for 1924–1960; 3, Porterfield (1980) for 1909–1959; 4, Ogden Beeman and Associates and Ray Krone and Associates (1992) for 1956–1990. Error bars on net-sedimentation rates and intertidal mudflat area are described in Section 5. Note that San Pablo Bay was erosional for the last.

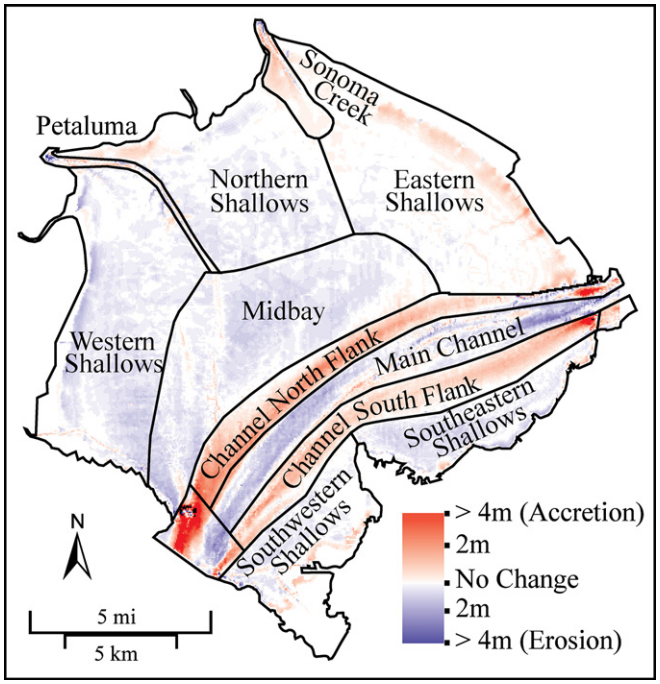

Fig. 5. Similar dynamical regions overlain on sedimentation in San Pablo Bay from 1951 to 1983. Regions were defined using the depth and patterns of erosion and deposition, which varied throughout the study.

Net-sedimentation rates in the 11 regions varied over time and, like net sedimentation for the entire bay, changed with sediment delivery to the bay. From 1856 to 1887, all regions except the Sonoma Creek ebb-tidal delta exhibited net deposition as large volumes of hydraulic-mining debris entered San Pablo Bay (Table 2). From 1951 to 1983, the most erosional period, some areas still had significant deposition (Table 2). The margins of the main channel (Channel North Flank and Channel South Flank) were depositional during all periods causing it to narrow (Figs. 2a, b and 3; Table 2). Channel deepening accompanied the narrowing during all periods except from 1856 to 1887 (Fig. 3). The eastern shallows were the only nonchannel region with net deposition during all periods. Net sedimentation in the shallows generally decreased throughout the study period (Fig. 6a).

The timing and pattern of net sedimentation in the shallows are important because of the relation between sedimentation in the shallows and intertidal mudflat area. From 1856 to 1887, the shallows exhibited net deposition (Fig. 6a) and intertidal mudflat area increased in all parts of San Pablo Bay (Fig. 6b). Net sedimentation in all the shallows decreased from 1887 to 1898, possibly because of a decrease in sediment delivery as hydraulic mining was abruptly stopped in 1884, by disequilibrium (unstable morphology), by diking of mudflats, or by a combination of these factors. Although net sedimentation decreased, the eastern shallows were still depositional.

The response of the intertidal mudflats reflected the net sedimentation in the shallows (Fig. 6a, b and 7). The intertidal mudflat area rapidly decreased after 1887 in the western part of the bay, was nearly stable in the northern and southeastern parts of the bay, and increased in the eastern part of the bay. During the last period (1951–1983), both net sedimentation in the shallows and intertidal mudflat area decreased in all regions of the bay (Fig. 6a, b).

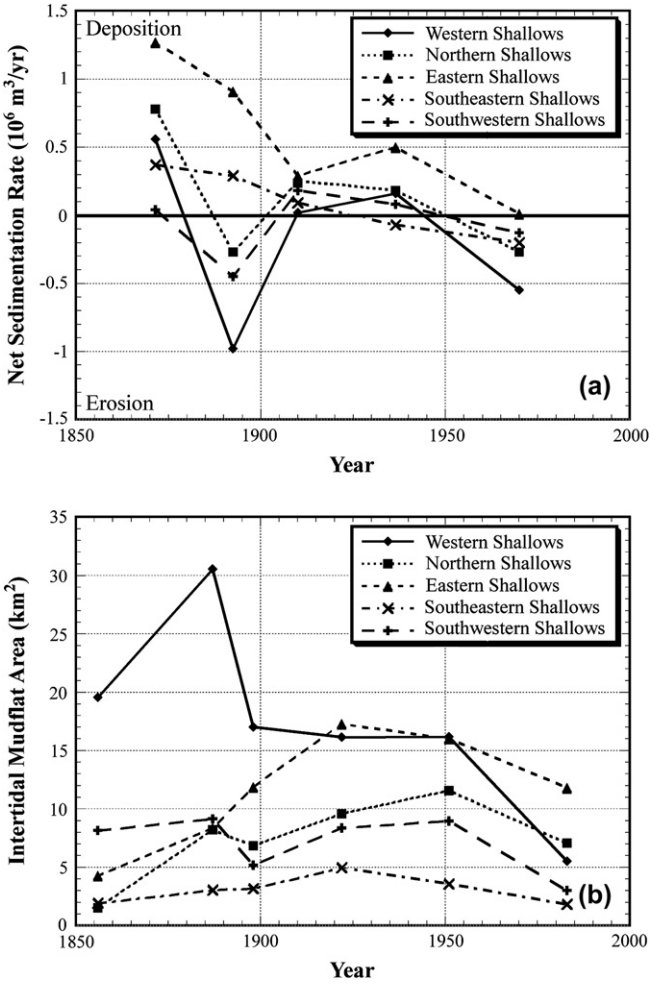

Fig. 6. Net-sedimentation rates in shallows (a) and intertidal mudflat area (b) by dynamical region.

6. Discussion

6.1. Does a simple model for sedimentation work?

The simple model (presented in Section 5.2) of sediment delivery from rivers controlling net sedimentation in San Pablo Bay assumes that other processes that deliver and remove sediment from San Pablo Bay are constant over time. This assumption can be examined in the sediment budget for San Pablo Bay (terms and connections shown in Fig. 8). The difference between the rate of sediment delivery from rivers and the net-sedimentation rate in San Pablo Bay, S_{SPB}, is given by

Table 2
History of net-sedimentation rates for dynamically similar regions in San Pablo Bay. Regions are defined in Fig. 5

Region	Net-sedimentation rate (cm/yr)				
	1856–1887	1887–1898	1898–1922	1922–1951	1951–1983
Western Shallows	0.6	−1.0	0.0	0.2	−0.5
Petaluma Channel	0.4	0.2	0.5	0.0	0.0
Northern Shallows	0.8	−0.3	0.3	0.2	−0.3
Sonoma Creek, ETD	−0.1	0.1	0.0	0.0	0.0
Eastern Shallows	1.3	0.9	0.3	0.5	0.0
Midbay	1.3	−0.6	0.3	0.7	−0.5
Channel North Flank	1.2	1.6	0.2	1.2	0.6
Main Channel	0.1	−0.1	−1.1	−1.0	−0.3
Channel South Flank	2.2	0.7	0.3	−0.1	0.4
Southwestern Shallows	0.0	−0.5	0.2	0.1	−0.1
Southeastern Shallows	0.4	0.3	0.1	−0.1	−0.2

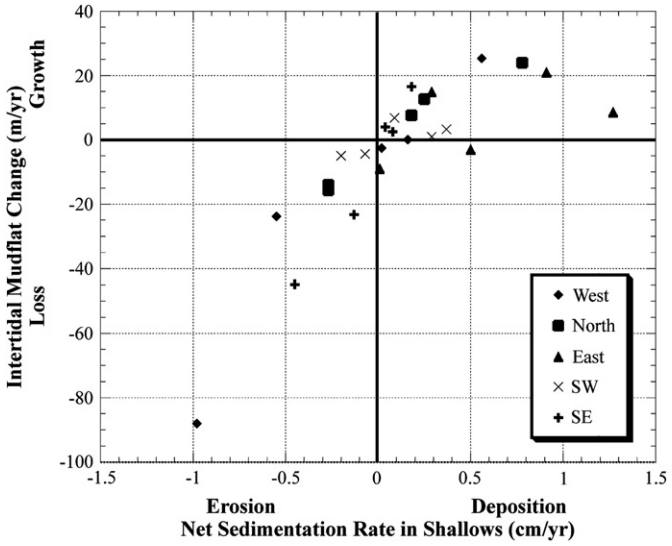

Fig. 7. Relation of net sedimentation in shallows (depth, $< \sim 1.8$ m, Fig. 5) and average intertidal mudflat width.

$$Q_{SSJ} + Q_L - S_{SPB} = S_D + S_{SBCS} + M_D + M_{SBCS} + M_{SPB} + E_{CS} + E_{CB} + BP - Q_{CBSPB} \quad (1)$$

where Q_{SSJ} is the sediment-delivery rate from the Sacramento and San Joaquin Rivers to the Delta, Q_L is the sediment-delivery rate from local streams (primarily Napa and Sonoma Creeks and the Petaluma River), S_D is the net-sedimentation rate in Delta channels and flood plains, S_{SBCS} is the net-sedimentation rate in the Suisun Bay region and Carquinez Strait, M_D is the sediment deposition rate in tidal marshes of the Delta, M_{SBCS} is the sediment deposition rate in tidal marshes of the Suisun Bay region and Carquinez Strait, M_{SPB} is the sediment deposition rate in tidal marshes of San Pablo Bay, E_{CS} is the rate that sediment eroded in San Pablo Bay is transported to Carquinez Strait, E_{CB} is the rate sediment eroded in San Pablo Bay is transported to Central San Francisco Bay, BP is the rate of sediment bypassing San Pablo Bay, and Q_{CBSPB} is the rate of sediment delivery from Central Bay to San Pablo Bay.

Eq. (1) can be simplified by neglecting small terms and those that are accounted for elsewhere. Assuming that marshes accrete to keep up with relative sea-level rise, the sediment deposition rates in marshes M_D, M_{SBCS}, and M_{SPB} are small relative to the other terms. For example in San Pablo Bay, the rate of deposition on marshes for 1856, when tidal-marsh extent was the largest (244 km^2, Van Royen and Siegel, 1959), was less than 0.4×10^6 m^3/yr (244 km^2 marsh $\times$ 1.4 mm/yr). Significant parts of the tidal-marsh area were reclaimed for agriculture by 1887 (Fig. 2a). Reclamation reduced tidal-marsh area in San Pablo Bay to 55 km^2 in 1980 (Dedrick, 1993). After 1887, M_{SPB} is a very small term in the budget, on the order of 0.1×10^6 m^3/yr. Similarly, M_D and M_{SBCS} have decreased over time. Tidal-marsh area in the Suisun Bay region decreased from 265 km^2 in 1800 to 55 km^2 in 1998 (Goals Project, 1999). Marsh deposition in the Delta, which decreased over time with levee building and diking, was likely a small term in the sediment budget after the late 1800s.

Although no estimates of E_{CS} have been published, flow measurements from Burau et al. (1993) at the west end of Carquinez Strait indicate that sediment eroded from San Pablo Bay is transported upestuary during neap tides when gravitational circulation results in upestuary near-bottom flows. During spring tides, flow and sediment transport are from Carquinez Strait to San Pablo Bay throughout the water column. Ganju and Schoellhamer (2006) used Acoustic Doppler Current Profiling (ADCP) and suspended concentration data to calculate suspended-sediment flux at the east end of Carquinez Strait, approximately 10 km from San Pablo Bay. At this location,

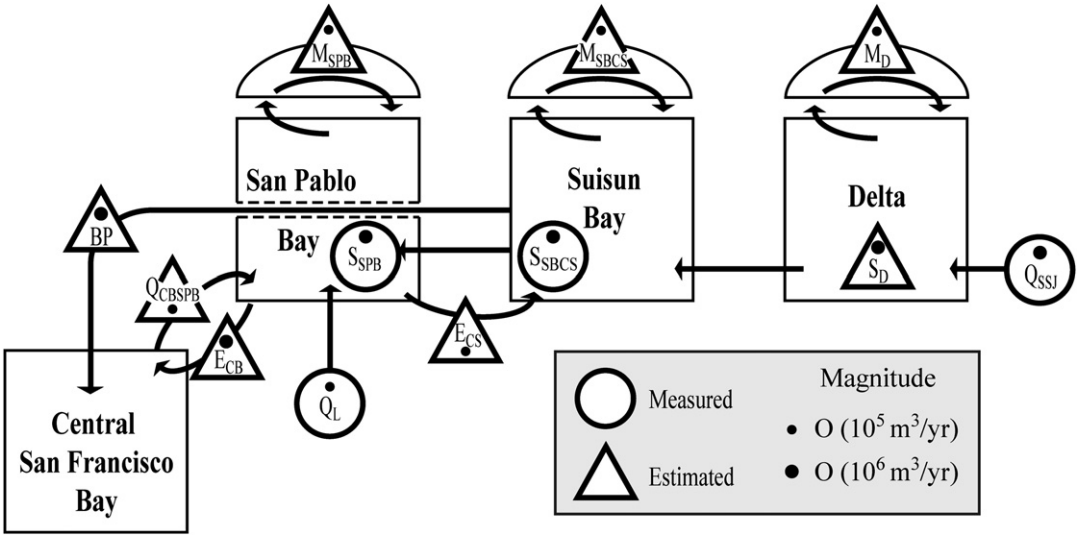

Fig. 8. San Pablo Bay sediment budget schematic. Arrows indicate direction of sediment exchange. Circles indicate measured sediment budget components. Estimated components are indicated by triangles. The order of magnitude for sediment volume rates is indicated by the size of the dot within the budget component. The notation used is Q is sediment delivery, S net sedimentation, M marsh deposition, E transport of eroded sediment, and BP is sediment bypassing.

suspended-sediment flux driven by gravitational circulation dominates during the dry months when there was a strong longitudinal salinity gradient. During the driest of years, the annual net suspended-sediment flux was upestuary. Fortunately, for balancing of the sediment budget, we need not estimate E_{CS} because it is accounted for in the net-sedimentation rates of Carquinez Strait, Suisun Bay and the Delta (if the sediment makes it that far).

Likewise, we need not account for upestuary sediment transport from Central Bay to San Pablo Bay, Q_{CBSPB}, because it is accounted for in the net-sedimentation rates of San Pablo Bay.

Neglecting small terms and those implicit in other terms and rearranging, Eq. (1) simplifies to:

$$BP + E_{CB} = Q_{SSJ} + Q_L - S_{SBCS} - S_{SPB} - S_D \quad (2)$$

To evaluate Eq. (2), we recalculated net-sedimentation rates for the same period as for river sediment-delivery estimates by weighting the rates listed in Table 1 with the percentage of time represented during each period (Table 3). The sum of the terms to the right of the equal sign, except for net sedimentation in the Delta (S_D), is well constrained by data and decrease over time (Porterfield, 1980; Cappiella et al., 1999; this analysis). S_D was accounted for in the 1850–1914 sediment-delivery estimate by Gilbert (1917) and assumed to be 1.0×10^6 m^3/yr thereafter based on estimates by Wright and Schoellhamer (2005) and Smith (1965).

E_{CB} is a potentially large term that can be estimated from the volumes of eroded and deposited sediment (Table 1) and the sediment delivery from rivers and the net sediment in the Delta, Suisun Bay, and Carquinez Strait (Table 3). The volume of eroded sediment is not equivalent to E_{CB} because (1) redeposition of eroded sediment in San Pablo Bay results in the volume of eroded sediment overestimating E_{CB}, and (2) new sediment replacing eroded sediment that was removed from San Pablo Bay results in the volume of eroded sediment underestimating E_{CB}. From 1956 to 1990, the minimum E_{CB} value (i.e., all eroded sediment redeposited in San Pablo Bay) is 0.7×10^6 m^3/yr (2.4×10^6 m^3/yr eroded minus 1.7×10^6 m^3/yr deposited; Table 1). The maximum E_{CB} value for this period, which occurs if all the sediment entering San Pablo Bay (from local streams, the Sacramento and San Joaquin Rivers, and net erosion from Suisun Bay and Carquinez Strait) were initially deposited, eroded, and removed from San Pablo Bay to the Central Bay is 5.1×10^6 m^3/yr (3.1×10^6 m^3/yr from rivers and local streams plus 1.3×10^6 m^3/yr from erosion of Suisun Bay and Carquinez Strait plus 1.7×10^6 m^3/yr deposited in San Pablo Bay minus 2.4×10^6 m^3/yr eroded from San Pablo Bay; Tables 1, 3). These estimates neglect losses to marshes, which are relatively small. Using this approach, the ranges of E_{CB} values for 1850–1914, 1909–1959, and 1924–1960 are $0–7.7 \times 10^6$, $0–6.6 \times 10^6$, and $0–5.7 \times 10^6$ m^3/yr; respectively. The averages of E_{CB} values during the periods 1850–1914, 1909–1959, 1924–1960, and 1956–1990 are 3.8×10^6, 3.3×10^6, 2.8×10^6, and 2.9×10^6 m^3/yr, respectively, yielding a grand average of 3.2×10^6 m^3/yr; the average E_{CB} value for the 1900s is 3.0×10^6 m^3/yr, an admittedly crude estimate of E_{CB}. Future research using sediment transport modeling could refine this estimate.

Assuming that $E_{CB} = 3.0 \times 10^6$ m^3/yr gives sediment bypassing rates of 4.9, 2.4, 1.3, and 1.1×10^6 m^3/yr for the periods 1850–1914, 1909–59, 1924–60, and 1956–90, respectively (Table 3). The decrease in BP during the study period is not unexpected. BP is scaled by the magnitude and frequency of floods. Larger floods transport more sediment through San Pablo Bay. This greater bypassing is caused both by stronger flows advecting sediment through the bay faster and higher sediment concentrations that commonly accompany stronger flows. More frequent floods increase cumulative sediment bypassing. Dams are designed to decrease both the magnitude and frequency of floods. With the increased damming of the Sacramento and San Joaquin Rivers and their tributaries, sediment bypassing of San Pablo Bay has likely decreased.

An additional factor to consider in sediment bypassing is that the relation between sediment concentration and flow magnitude (sediment–discharge rating curve) for rivers feeding San Pablo Bay is also changing. Wright and Schoellhamer (2004) showed that, for the same flow, the sediment concentration (and, thus, sediment transport) decreased for the Sacramento

Table 3
Major terms in sediment budget for San Pablo Bay (terms also shown in Fig. 8). Erosional loss from San Pablo Bay to Central San Francisco Bay, E_{CB}, is assumed to be constant over time and assigned a rate of 3.0×10^6 m^3/yr. Sediment from the Sacramento and San Joaquin Rivers bypassing San Pablo Bay (primarily during floods), BP, is calculated to balance the sediment budget. When a constant rate of erosional loss of sediment from San Pablo Bay is assumed, sediment bypassing decreases as sediment delivery decreases, which is the expected relation

Period	Sediment delivery from rivers $Q_{SSJ} + Q_L$ (10^6 m^3/yr)	Net sedimentation upestuary[a] $S_{SBCS} + S_D$ (10^6 m^3/yr)	Net sedimentation in San Pablo Bay S_{SPB} (10^6 m^3/yr)	San Pablo Bay loss[b] E_{CB} (10^6 m^3/yr)	Sediment bypassing BP (10^6 m^3/yr)
1850–1914	14.1	1.0	5.2	3.0	4.9
1909–1959	6.2	−0.8	1.6	3.0	2.4
1924–1960	5.0	−0.9	1.6	3.0	1.3
1956–1990	3.1	−0.3	−0.7	3.0	1.1

[a] Net sedimentation in the Delta, S_D, is accounted for in the 1850–1914 sediment-delivery estimate (Gilbert, 1917) and assumed to be 1.0×10^6 m^3/yr thereafter based on estimates by Wright and Schoellhamer (2005) and Smith (1965).

[b] E_{CS}, erosional loss from San Pablo Bay to Carquinez Straits and Suisun Bay is accounted for in S_{SBCS}; Q_{SSJ}, sediment delivered from the Sacramento and San Joaquin Rivers at the entrance to Suisun Bay; Q_L, sediment delivered from local streams; S_{SBCS}, change is sediment storage in the Suisun Bay area and Carquinez Strait; E_{CB}, erosional loss (flux of eroded material) from San Pablo Bay to Central San Francisco Bay; BP, sediment from the Sacramento and San Joaquin Rivers that bypasses San Pablo Bay.

River from 1957 to 2001. The Sacramento River contributes 80–90% of the sediment to the bay (Porterfield, 1980). Assuming sediment concentrations are not greatly modified when traveling from the river source to San Pablo Bay, this change in the sediment–discharge rating curve also would contribute to a decrease in BP.

The magnitude and trend of sediment bypassing rates, though reasonable, are only estimates and strongly depend on estimates of the rate at which eroded sediment is removed from San Pablo Bay. If this rate has decreased (or increased) over time, the above analysis would predict a corresponding equal increase (or decrease) in sediment bypassing.

In summary, a strong correlation exists between sediment-supply and net-sedimentation rates in San Pablo Bay (Fig. 4a), complicated, however, by uncertainty in sediment bypassing and sediment removal rates, two large terms in the sediment budget that have likely changed over time. Past sediment-supply and net-sedimentation rates are consistent with a constant (at the decadal time scale) sediment removal rate and sediment bypassing that has decreased over time. However, this solution is not a unique balance of the sediment budget. To increase our ability to predict net sedimentation, we must improve our understanding of the processes that cause bypass and removal of sediment from San Pablo Bay.

6.2. Sediment transport and redistribution within San Pablo Bay

Another level of prediction desired is the response of different parts of San Pablo Bay to fluctuations in sediment delivery. To be able to predict this response, we need to understand sediment redistribution within the bay. The data presented in Section 5.4 indicate significant sediment redistribution from the western and/or northern shallows to the eastern shallows.

Spatial and temporal trends in net sedimentation in the shallows (Figs. 2b and 6a) indicate that, for all periods, net deposition in the eastern shallows is greater than in the western or northern shallows. Interestingly, all the shallows except those in southeastern part of San Pablo Bay have similar trends in net sedimentation over time, regardless of becoming more erosional or depositional, but are offset by a constant. One explanation for this offset is that sedimentation scales with sediment delivery, with an overlay of redistribution from the western or northern shallows to the eastern shallows. This combination results in net sedimentation rates that parallel each other and are offset in magnitude after accounting for redistribution from the western shallows to the eastern shallows, mimicking observed behavior (Fig. 6a). Mechanisms for sediment redistribution from west to east are asymmetric tidal currents, with stronger flood-tide currents advecting more sediment to the east (Klingeman and Kaufman, 1965, Fig. 23) and currents generated by westerly or southwesterly winds advecting sediment to the east.

6.3. Future conditions

The morphology of San Pablo Bay will not return to that of 1856. The great influx of sediment during the hydraulic-mining period resulted in deposition that changed morphology significantly, which, in turn, changed sediment transport patterns. Adding to this perturbation to the system was diking of tidal marshes that reduced the tidal prism and resulted, for example, in filling of channels offshore of the Petaluma River (Ganju et al., 2004 presents a conceptual model for exchange of sediment between San Pablo Bay and the Petaluma River).

Generally, San Pablo Bay will continue to erode in the near term unless its sediment delivery increases. An increase in sediment delivery is not likely with damming and water projects acting to decrease sediment delivery. The eastern shallows, which are more depositional than the other shallows, will be the last area to become erosional. The effects of sea-level rise on deposition and erosion in San Pablo Bay are unknown. A decrease in bottom shear-stress from the increase in depth in the shallower portions of the bay decreasing wave orbital velocities is expected to favor deposition, but the degree that this effect will be counteracted by changes in the magnitude and pattern of tidal currents is hard to predict without the use of a coupled hydrodynamic/sediment transport model.

The main channels will likely continue to narrow and deepen. The main channel has been narrowing and deepening since 1887, and we expect this trend to continue. We speculate that the channel deepening response was initiated by channel narrowing from high sediment loads during the hydraulic-mining period. Narrowing may have sufficiently altered bottom shear-stress distributions so that deepening was easier than widening to accommodate flow. This hypothesis may be tested by applying a three-dimensional hydrodynamic and sediment transport model. Channel evolution could be modified by restoration of tidal mashes upestuary. Restoration would result in a greater tidal prism and increased flow through the main channel and could change sedimentation rates and patterns. Sea-level rise will affect channel geometry to the degree that it alters the tidal prism.

How San Pablo Bay evolves will be important to not only its health (e.g., habitat change) but that of San Francisco Bay as a whole. For example, San Pablo Bay contains more than 100×10^6 m^3 of hydraulic-mining debris with an average mercury concentration from 0.3 to 0.6 ppm (Jaffe et al., 1999). Erosion of this sediment will release tens of thousands of grams of mercury to the water column that could be transported throughout the San Francisco Estuary. Future conditions of San Pablo Bay will also affect tidal-marsh-restoration efforts. If San Pablo Bay continues to erode, more sediment will be needed for restoration because sediment will be required not only for the creation of tidal marshes but also for the expansion of intertidal mudflats and shallows that coexist with marsh.

7. Conclusions

Quantitative analysis of historical hydrographic surveys has been used to learn how San Pablo Bay has changed since the Gold Rush and what processes were key in causing this change. It is concluded that:

1. The morphology of San Pablo Bay changed drastically from 1856 to 1983. In 1856, San Pablo Bay had a complex morphology, with a broad main channel, side channels, and an ebb-tidal delta crossing the shallower parts of the bay. In 1983, all the channels except the main channel had filled, and erosive processes planed the shallows, creating uniform, gently sloping surfaces.
2. Human activities that changed sediment delivery from rivers were a primary control on sedimentation and the evolution of San Pablo Bay. From 1856 to 1887, $259 \pm 14 \times 10^6$ m^3 of sediment was deposited in San Pablo Bay, coinciding with a high rate of sediment delivery (14.1×10^6 m^3/yr) to San Francisco Bay during the hydraulic-mining period. In contrast, from 1951 to 1983, $23 \pm 3 \times 10^6$ m^3 of sediment was eroded from San Pablo Bay as the rate of sediment delivery from the Sacramento and San Joaquin Rivers decreased to about 3×10^6 m^3/yr.
3. Intertidal mudflat area and distribution changed throughout the study period. In 1887, intertidal mudflat area was at a maximum (60.6 ± 6.6 km^2). Intertidal mudflat area had decreased to a minimum (31.7 ± 3.9 km^2) in 1983. In 1856, intertidal mudflats were largest in the western part of San Pablo Bay, but have since become more evenly distributed.
4. Intertidal mudflat area is related to sedimentation on the shallows (<1.8-m depth), reflecting sediment delivery to the bay. Intertidal mudflat area was largest after the unusually high influx of sediment from hydraulic mining resulted in building of the shallows and intertidal mudflats, and smallest in 1983 after damming decreased sediment delivery.
5. The simple model that sediment delivery controls net sedimentation explains much of the sedimentation trend in San Pablo Bay. This model predicts that erosion will increase in the future if sediment delivery continues to decrease.

Acknowledgments

This research was supported by the U.S. Geological Survey's Priority Ecosystem Science study of San Francisco Bay. Laura Zink Torresan digitized historical hydrographic and topographic surveys. The manuscript was improved by reviews from Dave Schoellhamer, Noah Snyder, and three anonymous reviewers.

References

Adams, K.T., 1942. Hydrographic Manual, revised ed. U.S. Department of Commerce, Coast and Geodetic Survey, Special Publication 143, 407 pp.

Burau, J.R., Simpson, M.R., Cheng, R.T., 1993. Tidal and residual currents measured by an acoustic Doppler current profiler at the west end of Carquinez Strait, San Francisco Bay, California, March to November 1988. U.S. Geological Survey Water-Resources Investigations Report 92-4064, 76 pp.

Cappiella, K., Malzone, C., Smith, R., Jaffe, B.E., 1999. Sedimentation and bathymetry changes in Suisun Bay: 1867–1990. U.S. Geological Survey Open-File Report 99-563. http://geopubs.wr.usgs.gov/open-file/of99-563/.

Cheng, R.T., Gartner, J.W., 1984. Tides, tidal and residual currents in San Francisco Bay, California – results of measurements, 1979–1980. U.S. Geological Survey Water-Resources Investigations Report 84-4399, 368 pp.

Conomos, T.J., Peterson, D.H., 1976. Suspended-particle transport and circulation in San Francisco Bay: An overview. In: Wiley, M. (Ed.), Estuarine Processes, vol. 2. Academic Press, New York, pp. 82–97.

Dedrick, K.G., 1983. Use of early hydrographic surveys in studies of California estuaries. Coastal Zone '83, pp. 2296–2316.

Dedrick, K.G., 1993. Atlas of present tidal marshlands, San Francisco Bay, California. Coastal Zone '93, pp. 2451–2463.

Friedrichs, C.T., 1995. Stability shear stress and equilibrium cross-sectional geometry of sheltered tidal channels. Journal of Coastal Research 11, 1062–1074.

Ganju, N.K., Schoellhamer, D.H., Warner, J.C., Barad, M.F., Schladow, S.G., 2004. Tidal oscillations of sediment between a river and a bay: a conceptual model. Estuarine, Coastal and Shelf Science 60, 81–90.

Ganju, N.K., Schoellhamer, D.H., 2006. Annual sediment flux estimates in a tidal strait using surrogate measurements. Estuarine, Coastal and Shelf Science 69, 165–178.

Gartner, J.W., Yost, B.T., 1988. Tides, and tidal and residual currents in Suisun and San Pablo Bays, California – results of measurements, 1986. U.S. Geological Survey Water-Resources Investigations Report 88-4027, 94 pp.

Gibbs, A.E., Gelfenbaum, G., 1999. Bathymetric change off the Washington-Oregon coast. Proceedings of Coastal Sediments '99, Long Island, N.Y., pp. 1627–1641.

Gilbert, G.K., 1917. Hydraulic mining debris in the Sierra Nevada. U.S. Geological Survey Professional Paper 105, 154 pp.

Goals Project, 1999. Baylands Ecosystem Habitat Goals. A Report of Habitat Recommendations Prepared by the San Francisco Bay Area Wetlands Ecosystem Goals Project. First Reprint. U.S. Environmental Protection Agency/S.F. Regional Water Quality Control Board, San Francisco, CA/Oakland, CA.

Hayes, T.P., Kinney, J.J., Wheeler, N.J., 1984. California Surface Wind Climatology. California Air Resources Board, Aerometric Data Division, 107 pp.

Higgins, S.A., Jaffe, B.E., Smith, R.E., 2005. Bathychronology: Reconstructing historical sedimentation from bathymetric data in a GIS, U.S. Geological Survey Open-File Report OFR-2005-1284, 19 pp. plus appendix. http://pubs.usgs.gov/of/2005/1273/.

Higgins, S.A., Jaffe, B.E., Fuller, C.C., 2007. Reconstructing sediment age profiles from historical bathymetry changes in San Pablo Bay, California. Estuarine. Coastal and Shelf Science 73 (1–2), 165–174.

Hopkins, D., List, J.H., Jaffe, B.E., Dalziel, K.A., 1991. Cartographic production for the Louisiana Barrier Island Erosion Study: 2. Generation of surface grids. U.S. Geological Survey Open-File Report 91-615, 28 pp.

Jaffe, B.E., List, J.H., Sallenger Jr., A.H., Holland, T., 1991. Louisiana Barrier Island Erosion Study: correction for the effect of relative sea level change on historical bathymetric survey comparisons, Isles Dernieres area, Louisiana. U.S. Geological Survey Open-File Report 91-276, 33 pp.

Jaffe, B.E., Smith, R.E., Torresan, L., 1998. Sedimentation and bathymetric change in San Pablo Bay, 1856–1983. U.S. Geological Survey Open-File Report 98-759. http://geopubs.wr.usgs.gov/open-file/of98-759/.

Jaffe, B.E., Smith, R.E., Cappiella, K., Bouse, R., Luoma, S., Hornberger, M., 1999. Mercury-Contaminated Hydraulic Mining Debris in North San Francisco Bay – A Legacy of the Gold Rush (abstract). Geological Society of America. Cordilleran Annual Section Meeting 31, no. 6, 66.

Klingeman, P.C., Kaufman, W.J., 1965. Transport of radionuclides with suspended sediment in estuarine systems. Berkeley, University of California, Sanitation Engineering Research Laboratory Report No. 65-15, 222 pp.

Krone, R.B., 1979. Sedimentation in the San Francisco Bay system. In: Conomos, T.J. (Ed.), San Francisco Bay, the Urbanized Estuary. Pacific Division of the American Association for the Advancement of Science, pp. 85–96.

List, J.H., Jaffe, B.E., Sallenger Jr., A.H., Williams, S.J., McBride, R.A., Penland, S., 1994. Louisiana Barrier Island Erosion Study, Atlas of sea floor changes from 1878 to 1989. U.S. Geological Survey Miscellaneous Investigations Map I-2150-B, 62 pp.

Locke, J.L., 1971. Sedimentation and foraminiferal aspects of the recent sediments of San Pablo Bay. M.S. thesis, San Jose State University, San Jose, CA, 100 pp.

Lyles, S.D., Hickman, L.E., Debaugh Jr., H.A., 1988. Sea Level Variations for the United States, 1855–1986. National Oceanic and Atmospheric Administration, Washington, DC, 182 pp.

Marvin-DiPasquale, M., Agee, J., Bouse, R., Jaffe, B., 2003. Microbial cycling of mercury in contaminated wetland and open-water sediments of San Pablo Bay, California. Environmental Geology 43 (3), 260–267.

McKee, L.J., Ganju, N.K., Schoellhamer, D.H., 2006. Estimates of suspended sediment entering San Francisco Bay from the Sacramento and San Joaquin Delta, San Francisco Bay, California. Journal of Hydrology 323, 335–352.

Miller, A., 1967. Smog and Weather – The Effect of the San Francisco Bay on the Bay Area Climate. San Francisco Bay Conservation and Development Commission, 40 pp.

Monismith, S.G., Kimmerer, W., Burau, J.R., Stacey, M.T., 2002. Structure and flow-induced variability of the subtidal salinity field in Northern San Francisco Bay. Journal of Physical Oceanography 32, 3003–3019.

National Oceanic and Atmospheric Administration, Geophysical Data System for Hydrographic Survey Data (GEODAS), CD, version 3.3.

National Oceanic and Atmospheric Administration, 1986. Tide Tables, West Coast of North and South America. National Oceanic and Atmospheric Administration, Rockville, MD.

Ogden Beeman and Associates, Ray Krone and Associates, 1992. Sediment budget study for San Francisco Bay. Final report prepared for U.S. Army Corps of Engineers, San Francisco District, under contract DACW07-89-D-0029, 25 pp.

Porterfield, G., 1980. Sediment transport of streams tributary to San Francisco, San Pablo, and Suisun Bays, California, 1909–1966. U.S. Geological Survey Water-Resources Investigations Report 80-64, 92 pp.

Putnam, J.A., 1947. Estimating storm-wave conditions in San Francisco Bay. EOS (American Geophysical Union Transactions) 28 (2), 271–278.

Ruhl, C.A., Schoellhamer, D.H., Stumpf, R.P., Lindsay, C.L., 2001. Combined use of remote sensing and continuous monitoring to analyze the variability of suspended-sediment concentrations in San Francisco Bay, California. Estuarine, Coastal and Shelf Science 53, 801–812.

Sallenger, A.H., Goldsmith, V., Sutton, C.H., 1975. Bathymetric comparisons: a manual of methodology, error criteria and techniques. Special Report in Applied Marine Science and Ocean Engineering (SRAMSOE) 66, 34 pp.

Schalowitz, A.L., 1964. Shore and sea boundaries. U.S. Coast and Geodetic Survey Publication 10-1, 2, 749 pp.

Schoellhamer, D.H., Schellenbarger, G.G., Ganju, N.K., Davis, J.A., McKee, L.J., 2003. Sediment dynamics drive contaminant dynamics. In: San Francisco Estuary Institute (SFEI) (Ed.), The Pulse of the Estuary: Monitoring and Managing Water Quality in the San Francisco Estuary. SFEI Contribution 74. San Francisco Estuary Institute, Oakland, CA, pp. 21–26.

Sherwood, C.R., Jay, D.A., Harvey, R.B., Hamilton, P., Simenstad, C.A., 1990. Historical changes in the Columbia River Estuary. Progress in Oceanography 24, 299–352.

Smith, B.J., 1965. Sedimentation in the San Francisco Bay system. In: Proceedings of the Interagency Sedimentation Conference, vol. 970. U.S. Department of Agriculture Miscellaneous Publication, pp. 675–708.

Swanson, R.L., 1974. Variability of tidal datums and accuracy in determining datums from short series of observations. National Oceanic and Atmospheric Administration Technical Report 64, 41 pp.

Uncles, R.J., Peterson, D.H., 1996. The long-term salinity field in San Francisco Bay. Continental Shelf Research 16, 2005–2039.

Van Rijn, L.C., 1993. Principles of Sediment Transport in Rivers, Estuaries, and Coastal Seas. Aqua Publications, Amsterdam, 715 pp.

Van Royen, W., Siegel, C.O., 1959. Future development of the San Francisco Bay area, 1960–2020. Report prepared for the U.S. Army Corps of Engineers, San Francisco District by Business and Defense Services Administration, U.S. Department of Commerce.

Wahba, G., 1990. Spline models for observational data. CBMS-NSF Regional Conference Series in Applied Mathematics. Society for Industrial and Applied Mathematics, Philadelphia.

Wright, S.A., Schoellhamer, D.H., 2004. Trends in the sediment yield of the Sacramento River, California, 1957–2001. San Francisco Estuary and Watershed Science (online serial) 2 (Issue 2, Article 2). http://repositories.cdlib.org/jmie/sfews/vol2/iss2/art2.

Wright, S.A., Schoellhamer, D.H., 2005. Estimating sediment budgets at the interface between rivers and estuaries with application to the Sacramento–San Joaquin River Delta, Water Resources Research 41, W09428. doi:10.1029/2004WR003753.